Sol-gel Synthesis and Characterization of $LiMn_{2-x}Cu_xO_4$ Spinels

CARMEN DORINA ARUXANDEI[1], NICOLETA CORNEI[1*], CRISTINA AMALIA HUŢANU[1], CRISTINA ELENA CIOMAGA[2], PETRISOR MUGUREL SAMOILA[1], ALEXANDRA RALUCA IORDAN[1], MIRCEA NICOLAE PALAMARU[1]

[1] "Al. I. Cuza" University of Iasi, Faculty of Chemistry, 1th Carol I, 700506, Romania

[2] "Al. I. Cuza" University of Iasi, Faculty of Physics, 1th Carol I, 700506, Romania

The spinel samples $LiMn_{2-x}Cu_xO_4$ (x = 0.05, 0.10, 0.15, 0.20) were obtained by sol-gel method. The structure was characterized by X-ray diffraction (XRD), scanning electron microscopy (SEM), and infrared spectroscopy (FT-IR). The $LiMn_{2-x}Cu_xO_4$ have a cubic structure with the space group of Fd-3m symmetry in which lithium and manganese ions occupy tetrahedral (8a) sites and octahedral (16d) sites, respectively, within a cubic close-packed oxygen array with oxygen ions in (32e) sites. The electrical properties of the samples were investigated using impedance spectroscopy at room temperature. Complex impedance representation, Cole-Cole diagram, presents a single component which is demonstrating the electrical homogeneity of the samples.

Keywords: spinel oxide, X-ray diffraction, electric properties

Spinel $LiMn_2O_4$ has been extensively studied as cathode materials for lithium secondary batteries due to several advantages such as ease of preparation, low cost, less toxic and environmental safety [1]. Lithium transition-metal oxides are promising candidates for the cathode materials of rechargeable lithium batteries because of their high voltage and large rechargeable capacities [2]. In particular, the spinel $LiMn_2O_4$, has several advantages such as low cost and low toxicity, so that many intensive investigations have been carried out [3]. It has been usually prepared by solid-state reaction consisting of mechanical mixing and extensive heating at high temperature [4]. However, the powders obtained by solid-state reaction have an irregular grain shape and larger grain size with broad distribution, which are critical to the capacity and cyclability of lithium batteries. Therefore, in order to overcome these disadvantages, various new techniques have been developed such as co-precipitation, ion-exchange, sol-gel [5], Pechini [6], melt-impregnation [7], citric acid gel [8] methods, etc. These processes have showed the feasibility for preparing $LiMn_2O_4$ as cathode materials for lithium secondary batteries.

The purpose of the present paper is to study the influence of the substitution of Mn with Cu on the phase composition and electric properties of $LiMn_{2-x}Cu_xO_4$ spinel powders.

Experimental part

The powders with chemical composition were prepared by sol-gel method using citric acid as chelating agent. The stoichiometric amounts of analytical reagents of $LiNO_3$, $Mn(NO_3)_2 \cdot 4H_2O$ and $Cu(NO_3)_2 \cdot 3H_2O$ were dissolved in an aqueous solution of citric acid (Aldrich, high purity) [9, 10]. The molar ratio of total metal ions to citric acid was 1:1 in the solution. Ammonium hydroxide was added slowly to this solution with constant stirring until a *p*H of 7 - 7.5 was achieved. The mixture nitrate - citric acid solution was heated at 80°C, with continuous stirring. After the evaporation of the water excess, a highly viscous gel has been obtained. Subsequently, the gel was ignited at 300°C to evolve the undesirable gaseous products, resulting in the formation of a foamy powder. To complete the spinel formation the powder was presintered at 400°C/3h, 500°C/3h, 600°C/3h, and sintered at 750°C/12 h. The synthesis procedure of the powders is described in the flowchart shown in the figure 1.

The sintered samples were investigated by XRD, to determine begining of the solid-state reaction and the phase composition. The XRD analysis was performed with a Huber diffractometer at room temperature with Cu $K\alpha 1$, λ = 1.54051Å radiation, data being handled by Chekcell, and Powder Cell Programs. The Mn-O, Mn-Mn distances have been calculated from the atomic coordinates in the unit cell and are at the basis of our further discussion. The infrared (FT-IR) transmission spectrum was collected on powder sample with a JASCO 660 Plus spectrophotometer in KBr pellets. The FT-IR spectrum was taken in the frequency range from 1000 to 400 cm^{-1}. The change in the particle morphology was observed using a field-emission scanning electron microscope JSM 5600 LV. The a. c. impedance measurements were performed using an Agilent E4980A impedance analyzer over the frequency range from 10 Hz to 10^6 Hz.

Results and discussions

The XRD patterns for $LiMn_{2-x}Cu_xO_4$ have shown that the samples are essentially in the single phase form with the cubic symmetry except the samples with x = 0.05 which contain an amount of foreign phase (fig. 2).

The cell parameters have been refined through the Chekcell program (table 1). It can be found that the diffraction patterns of all samples have characteristic of spinel crystal structure (S.G. Fd-3m), in which lithium ions occupy the (16a) positions of tetrahedra, manganese ions (Mn^{3+} and Mn^{4+}) occupy the (16d) positions of octahedra and oxygen ions occupy the (32e) positions, tetrahedral and octahedral sites [11]. The similar diffraction patterns of spinel structure for the samples with doping indicate that the doped copper has entered the lattice of 16d positions to replace manganese. However, for the sample with x = 0.05 the reaction is not complete at this temperature because the XRD patterns show that contains a mixture of two phases: spinel structure and an amount of α-Mn_2O_3 respectively (fig. 2 and table 1).

It can be seen from table 1 that the cell constant, the volume and the bond length of spinel lithium manganese

* *email: ncornei@uaic.ro; Tel.: 02 32 20 11 36*

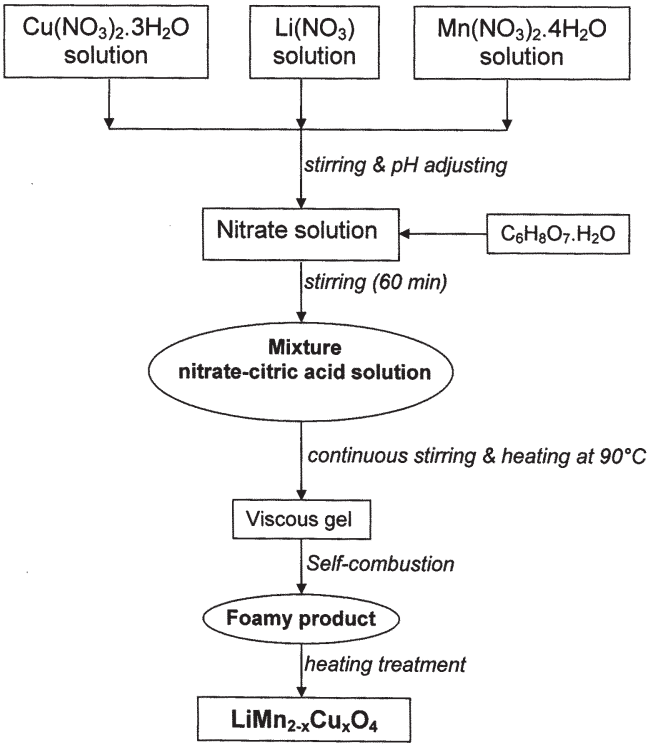

Fig. 1. Flowchart of the powders preparation

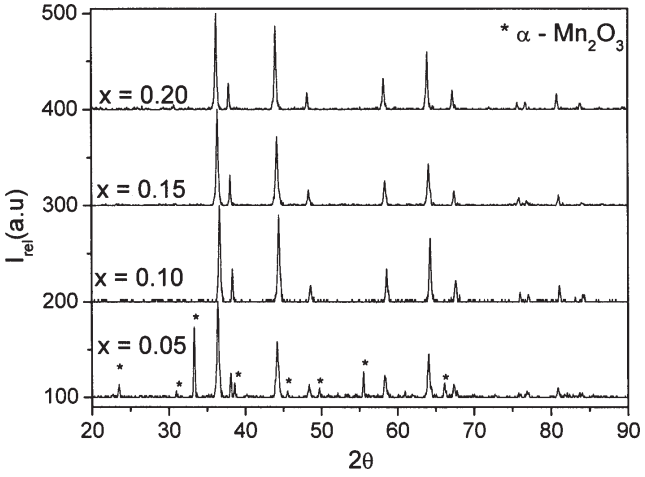

Fig. 2. XRD pattern of the $LiMn_{2-x}Cu_xO_4$ samples

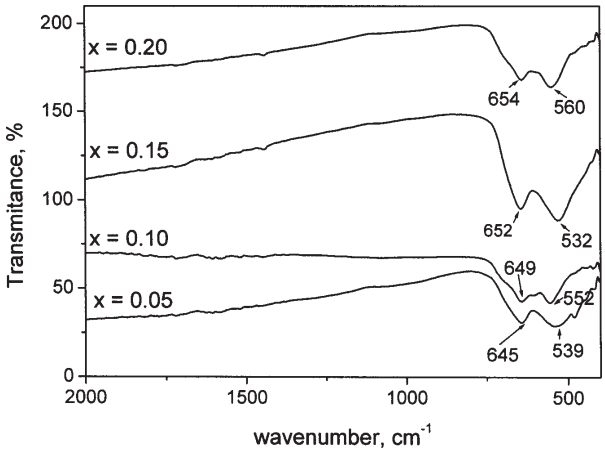

Fig. 3. FT-IR spectrum of $LiMn_{2-x}Cu_xO_4$ (x = 0.05, 0.10, 0.15, 0.20) sintered at 750°C.

Chemical composition	a (Å)	V (Å ^{3})	d_{Mn-Mn} (Å)	d_{Mn-O} (Å)	(%)* α-Mn_2O_3
$LiMn_{1.95}Cu_{0.05}O_4$	8.2384	559.150	2.9127	1.9439	27
$LiMn_{1.9}Cu_{0.1}O_4$	8.2328	558.011	2.9107	1.9426	0
$LiMn_{1.85}Cu_{0.15}O_4$	8.2199	555.392	2.9062	1.9395	0
$LiMn_{1.8}Cu_{0.2}O_4$	8.2133	554.055	2.9038	1.9380	0

Table 1
CELL PARAMETERS OF SPINEL SAMPLES WITH CHEMICAL COMPOSITION $LiMn_{2-x}Cu_xO_4$

oxide become small due to the doping of copper and decrease as the copper contents increase, indicating that spinel cell of lithium manganese oxide is contracted due to the doping of copper. This effect can be ascribed to the stronger bond of Cu-O than that of Mn-O.

Infrared technique has been employed to understand the metal-oxygen bond in the sintered powders. Figure 3 shows the FTIR spectrum of the samples.

From the FTIR spectra it has been observed that the strong frequency bands at 640-660 and 520-560 cm^{-1}, are responsible for the formation of $LiMn_{2-x}Cu_xO_4$. They are assigned to the asymmetric stretching of MnO_6 [12- 14]. Julien and Massot attributed the asymmetric stretching vibrations of MnO_6 octahedra bands with wavelengths of 504 and 617 cm^{-1}. They assigned the bands move higher wave numbers with increasing crystallite size or with increasing time of grinding of precursors [12]. In our samples the maximum absorption bands shift to higher frequency (from 617 and 504 cm^{-1}, respectively to 638 and 540 cm^{-1} respectively). This increase can be due to the presence of impurity phases, conditions of sintering and particle size, respectively. The impurity phases are confirmed by X-ray diffraction for samples with x = 0.05. The presence of Cu^{2+} ions on the B places determine an increase of degree of covalent Mn-O bonds which can be determined by the increase of Mn^{4+} concentration. This increase leads to a shift of peaks to higher frequency with increase of Cu concentration in the samples.

The microstructure and morphology play an important role in determining dielectric properties and these were examined by a high resolution scanning electron microscope. SEM images are shown in figure 4. Each powder is characterized by porous structure and submicron grains.

For $LiMn_{1.85}Cu_{0.15}O_4$ spinel we can observe submicron grains, a uniform grain size distribution (fig. 5) and the absence of the grain agglomerates. In the samples analyzed, there is a better distribution of the granules in the

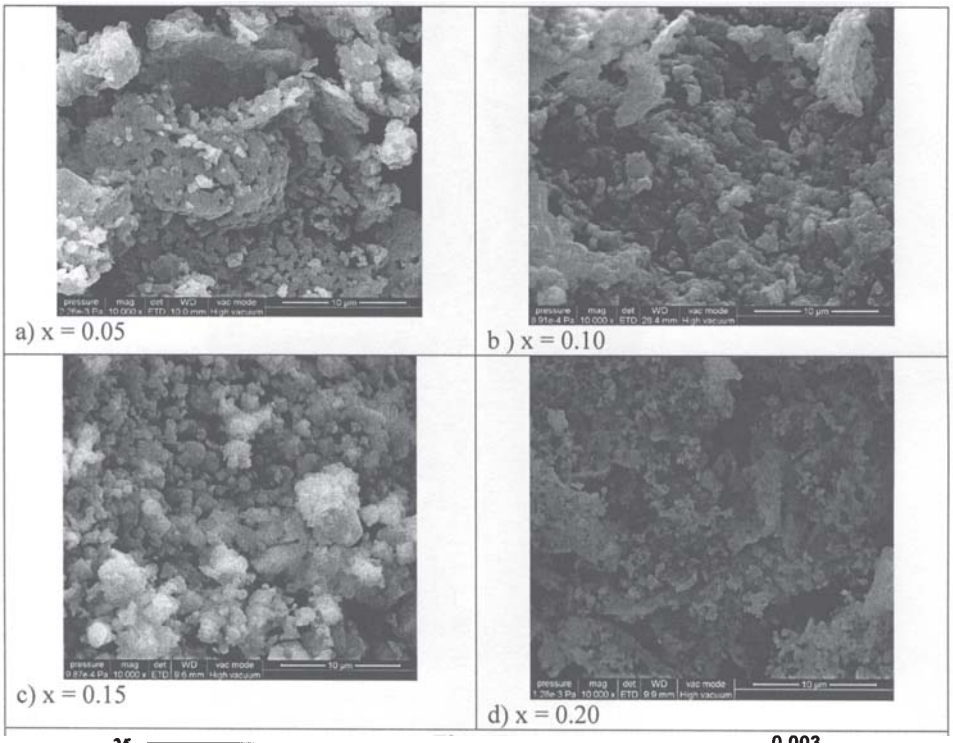

Fig. 4. SEM for $LiMn_{2-x}Cu_xO_4$ samples: a) x = 0.05; b) x = 0.10; c) x = 0.15; d) x = 0.20

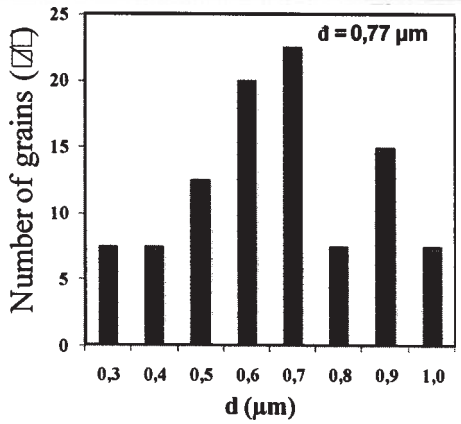

Fig. 5. Particle size distribution for $LiMn_{1.85}Cu_{0.15}O_4$

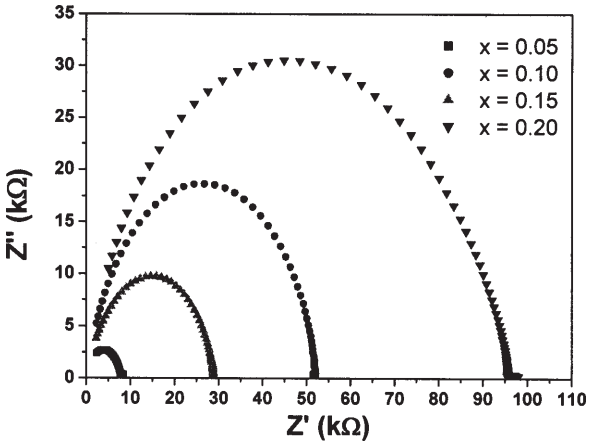

Fig. 6. Cole –Cole diagrams of $LiMn_{2-x}Cu_xO_4$ (x = 0.05, 0.10, 0.15, 0.20) at room temperature

range 0.2 to 1.1 µm. In other papers, it is worth noting that substitution of manganese with copper leads to higher average width of the granules.

The complex impedance plot (fig. 6) demonstrates a good homogeneity of the dielectric and conductive properties of the $LiMn_{2-x}Cu_xO_4$ samples. The impedance spectrum is characterized by single semicircular arcs, whose pattern changes with composition, indicating a modification of the resistance/reactance ratio when increasing the Cu addition *x*. A shift of the semicircle center

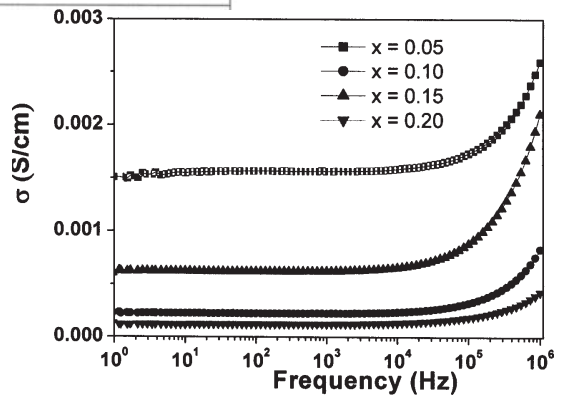

Fig. 7. Frequency dependencies of the electrical conductivity of $LiMn_{2-x}Cu_xO_4$ (*x* = 0.05, 0.10, 0.15, 0.20) at room temperature

from the origin of the complex plane plot takes place as result of the increasing dc-conductivity when the Cu concentration is higher. The bulk resistivity of the $LiMn_{2-x}Cu_xO_4$ ceramics increase from 2.4 x 10^3 Ω (for x = 0.05) to 5 x10^3 Ω (for x = 0.20).

Measurements of electrical conductivity in the range of frequency of 1-10^6 Hz are presented in the figure 7. The $LiMn_{2-x}Cu_xO_4$ ceramics show a decreasing of conductivity with addition of Cu.

The high values of σ ~ 1.5 x 10^{-3} S/cm of the samples in the investigated frequency range are demonstrating the semiconducting behaviour. A general condition for semiconducting behaviour is that the transition-metal ion could exhibit several valence states so that the electron hopping from low to high valence state can take place, i.e. Mn^{3+} and Mn^{4+} in the case of $LiMn_20_4$. Experimental data are usually discussed in terms of small-polaron transport theory for the electrical conductivity in transition metal oxides [15-16].

Conclusions

The samples with chemical composition $LiMn_{2-x}Cu_xO_4$ were obtained by sol-gel method using citric acid as chelating agent. The samples sintered at 750°C contain a single phase with a spinel structure except the sample with x = 0.05 which contain a small amount of α-Mn_2O_3.

The volume of the unit cell decrease with increase of Cu concentration due to an increase of the Mn^{4+} ions in the samples. SEM characterizations and ac dielectric properties of $LiMn_{2-x}Cu_xO_4$ (x = 0.05, 0.10, 0.15, 0.20) spinels oxides were studied. All powders were characterized by porous structure and submicron grains. The dielectric studies indicate that these compounds are ionic conductors at room temperature in the frequency range 10- 10^5 Hz .

The conductivity results also show that the $LiMn_{2-x}Cu_xO_4$ has a slight higher conductivity than $LiMn_20_4$ cathode material. The semiconducting behaviour could be explained in terms of small-polaron transport. It was suggested that the $LiMn_{2-x}Cu_xO_4$ spinel oxide could be developed for use in lithium-ion batteries.

Acknowledgements: This work was financial supported by POSDRU/89/1.5/S/63663 project.

References

1. SHOKOOHI, F. K., TARASCON, J. M., GUYOMARD, D., ITE-JECS Press, Inc., **14**, 1995, p 173
2. HE, J., LI, J., JIANG, C., WAN, C., Mater.Chem Phys. **95**, 2006, p 105
3. WU,M., ZHANG, Q., LU, H., CHEN, A., Solid State Ionics **169**, 2004, p 47
4. ENDRES, P., FUCHS,B., SACK, S.K., BRANDT, K., BECKER, G. F., PRAAS, H. W., Solid State Ionics **89** ,1996, p 221
5. LIU, W., KOWAL, K., FARRINGTON, G. C., J. Electrochem. Soc. **143**, 1996, p 3590
6. LIU, W., FARRINGTON, G. C., CHAPUT, F., DUNN, B., J. Electrochem. Soc. **143**, 1996, p 879
7. XIA, Y.Y., TAKESHIGE, H., NOGUCHI, H., YOSHIO, M., J. Power Sources **56**, 1995, p 61
8. SURYAKALA, K., MARIKKANNU, K.R., PARUTHIMAL KALAIGNAN, G., VASUDEVAN, T., Int. J. Electrochem. Sci., **3**, 2008, p136
9. PERIANU, E.A., GORODEA, I.A., PRIHOR, F., MITOSERIU, L., IANCULESCU,A.C., IORDAN, A.R., PALAMARU, M.N., Rev. Chim. (Bucharest), **61,** no. 2, 2010, p.242
10. POPOVICI, D., BOLOCAN, I., MATEI, V., MATEI, D., BOMBOS, D., DUSESCU, C., Rev. Chim. (Bucharest), **59,** no. 1, 2008, p.88
11. BERG, H., THOMAS, J.O. , WEN, L., FARRINGTON, G. C., Solid State Ionics, **112**, 1998, p 165
12. JULIEN, C.M., MASSOT, M., Ionics, **11**, 2005, p 226
13. HELAN, M., BERCHMANS, L.J., HUSSAIN, A. Z., Ionics, **16**, 2010, p 227
14. LAGASHETTY, A., HAVANOOR,V., BASAVARAJA, S., VENKATARAMAN, A., Indian J. of Chemical Technology, **15**, 2008, p 41
15. JULIEN, C., GENDRON, F., ZIOLKIEWICZ, S., NAZRI, G.A., Mater. Res. Soc. Symp. Proc. **548**, 1999, p 187
16. GOODENOUGH, J.B., MANTHIRAN, A., Wnetrzewski, B., J. Power Sources, **269**, 1993, p 43

Manuscript received: 5.03.2011